SERIES SOLUTION OF LAPLACE PROBLEMS

LLOYD N. TREFETHEN[1]

Abstract

At the ANZIAM conference in Hobart in February 2018, there were several talks on the solution of Laplace problems in multiply connected domains by means of conformal mapping. It appears to be not widely known that such problems can also be solved by the elementary method of series expansions with coefficients determined by least-squares fitting on the boundary. (These are not convergent series; the coefficients depend on the degree of the approximation.) Here we give a tutorial introduction to this method, which converges at an exponential rate if the boundary data are sufficiently well-behaved. The mathematical foundations go back to Runge in 1885 and Walsh in 1929. One of our examples involves an approximate Cantor set with up to 2048 components.

1 Introduction

I am a card-carrying conformal mapper [22], but it is my view that conformal mapping is usually not the best strategy for solving Laplace problems in multiply connected regions. The trouble is that the conformal mapping problem is typically as difficult as the original Laplace problem, or more so, because it may require resolution of geometric issues that are absent from the original problem. The aim of this paper is to give a tutorial introduction to the simple alternative of solving Laplace problems by series expansion with least-squares matching of boundary data. Nothing here is mathematically new, though these methods are not as well-known as they might be.

An important tool in connection with multiply connected conformal mapping is the Schottky–Klein prime function [15, 16, 29, 43], which gives considerable insight into the structure of such a map. If the prime function is known for a particular domain, then it can be used to solve certain Laplace problems [13, 14]. However, the prime function itself can only be computed numerically, and in fact, one of the best

―――――――――
[1]Mathematical Institute, University of Oxford, Oxford OX2 6GG, UK;
e-mail: trefethen@maths.ox.ac.uk.

methods for computing it makes use of the same kind of series expansions reviewed here [15, 17]. All in all, though the idea of solving multiply connected Laplace problems by conformal mapping is an old one—a book on such matters was published 30 years ago by Prosnak [47]—this approach is computationally unnecessary.

The aim of this paper is to show how series expansion methods can be used. It is structured in a tutorial fashion, treating a succession of problems, with MATLAB code listings given in the Appendix. These codes, which are descendants of codes in the unpublished essay [55], are an essential part of the presentation, and they include details that are not spelled out in the text.

For concreteness, most of the problems take the form of the computation of a Green function with its logarithmic singularity at the origin. This amounts to the computation of the harmonic measure [28, 48], that is, the function that determines the probability density that a particle undergoing Brownian motion from the origin will first encounter the boundary at each particular point. We also give a few examples illustrating how other kinds of Laplace problems, involving nonconstant boundary conditions for example, can be treated by the same approach. Although we do not show an example, the same methods can be applied for Neumann or Robin as for Dirichlet boundary conditions.

Many people have discovered versions of these ideas over the years, and I doubt anyone has a comprehensive understanding of the literature. Some references are given in Section 7, starting with Runge's theorem of 1885.

2 Green function for a disk

We begin with a problem that could be solved analytically. What is the Green function $u(z)$ in the exterior of a disk of radius r centred at position $z = c$ in the complex plane? Specifically, we seek a function u satisfying

$$\Delta u = 0, \quad u(z) = 0 \quad \text{for } |z - c| = r, \quad u(z) \sim \log|z| \quad \text{as } z \to 0 \qquad (2.1)$$

in the region of the complex plane exterior to $z = 0$ and the circle $|z - c| = r < |c|$, with regular behaviour at $z = \infty$, that is, $u(z) \to u_\infty$ as $z \to \infty$ for some constant u_∞. (For simplicity, we have omitted the factor $1/2\pi$ that would often appear in the definition of the Green function.) Throughout this paper, we regard the plane as either real or complex according to convenience. Thus the function $\log|z|$ in (2.1), for example, is a real function in the x–y plane that has been expressed for simplicity in terms of the complex variable $z = x + iy$.

To solve (2.1), we approximate u by a series expansion

$$u(z) = \log|z| - \log|z - c| + C + \sum_{k=1}^{N}[a_k \operatorname{Re}((z - c)^{-k}) + b_k \operatorname{Im}((z - c)^{-k})], \qquad (2.2)$$

which could be written in real form as

$$u(z) = \log|z| - \log r + C + \sum_{k=1}^{N} r^{-k}[a_k \cos(k\theta) - b_k \sin(k\theta)]$$

with $z - c = re^{i\theta}$. The coefficients a_k and b_k are chosen to satisfy $u(z) = 0$ as nearly as possible in a least-squares sense at $\texttt{npts} \gg N$ sample points along the boundary. The term $\log|z - c|$ is needed to make u regular as $z \to \infty$. (One could alternatively use $\log|z - \tilde{c}|$ with $\tilde{c}$ equal to a different point in the interior of the disk.) Note that only negative powers of $z - c$ appear in the series, because the domain is unbounded. Since the functions in play are analytic and the boundaries are smooth, geometric convergence occurs as a function of N, and a modest value like $N = 10$ is more than enough for plotting accuracy.

The MATLAB code $\texttt{disk1}$ computes the solution of (2.1) and plots contour lines for the particular choices $c = 3 + i$ and $r = 1$. Here as in all our codes, we strive to make the computational first half compact but legible, following the philosophy of "ten digit algorithms" [55]. Here is that first half of $\texttt{disk1}$:

```
% disk1.m    Green function exterior to a disk
%
% We seek the function u(z) that is zero for |z-c| = r and harmonic outside this
% circle, including at z=infty, except with u(z)~log|z| as z->0.  u is expanded as
%
%   u(z) = log|z| - log|z-c| + a(1)
%               + SUM_{k=1}^N a(2k)*real((z-c)^(-k)) + a(2k+1)*imag((z-c)^(-k)) .

c = 3+1i; r = 1;                    % center and radius of disk
N = 10; npts = 3*N;                 % no. expansion terms and sample pts
z = c + r*exp(2i*pi*(1:npts)'/npts);    % sample points
rhs = -log(abs(z)) + log(abs(z-c));     % right-hand side
A = ones(npts,2*N+1);
for k = 1:N                         % set up least-squares matrix
  A(:,2*k  ) = real((z-c).^-k);
  A(:,2*k+1) = imag((z-c).^-k);
end
a = A\rhs;                          % solve least-squares problem
```

The second half of each code, devoted to plotting, has been made extremely compact and is not very legible; see the Appendix.

The level curves computed by $\texttt{disk1}$ are shown in Figure 1. As a check of accuracy, we find by computing with larger values of N that the arbitrary value $u(2) \approx -0.5893274981708$ is accurate to four digits with $N = 4$, to seven digits with $N = 8$, and to 10 digits with $N = 12$. (Rigorous estimates can be based on the maximum principle; see Section 8.) All three computations, including plotting, take much less than a second on a laptop.

It is worth emphasizing that the series in (2.2), like all our series, is not made from Taylor or Laurent coefficients, which would be independent of N and could achieve convergence as $N \to \infty$ only in restricted regions of the plane. The coefficients in (2.2) depend on N, and they allow convergence irrespective of the shape of any region of analyticity or harmonicity. This situation is analogous to the well-known effect that on the real interval $[-1, 1]$, an analytic function f can be approximated by degree N polynomials with geometric convergence as $N \to \infty$, but these cannot be Taylor polynomials unless f is analytic in a disk of radius >1 [56].
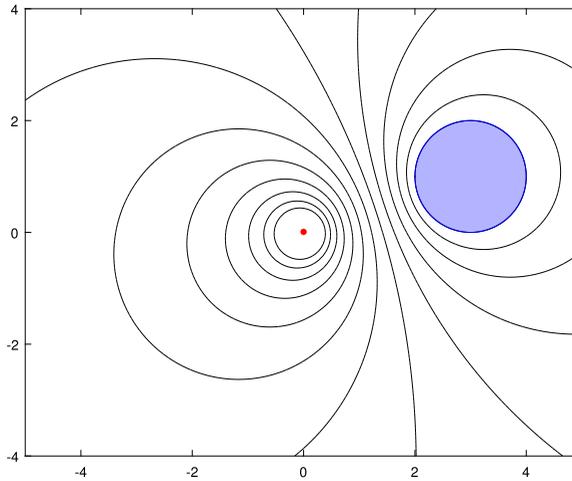
FIGURE 1. Green function $u(z)$ outside a disk computed with `disk1`. The level curves are regularly spaced between 0 on the boundary of the disk and $-\infty$ at the singularity at $z = 0$.

The curves in Figure 1 are equipotentials $u(z) = $ const, and as always with harmonic functions, it is also interesting to examine an orthogonal system of curves corresponding to streamlines. Among other benefits, these give a visual indication of harmonic measure along the boundary of the circle.[1] For this simple example, we could compute the orthogonal system just as level curves of the imaginary part of the same expansion. For multiply connected domains, however, that approach leads to headaches of tracking branches of the complex logarithm. A simpler alternative is to compute the orthogonal curves by solving an ordinary differential equation (ODE) to climb the gradient,

$$\frac{dz}{dt} = \frac{\nabla u}{\|\nabla u\|}, \tag{2.3}$$

starting from points close to the singularity at $z = 0$ and equally spaced around it. The gradient can be computed by taking advantage of the complex variables interpretation to note that if f is a complex analytic function, then the gradient of its real part is given (in the form of a vector represented as a complex number) by

$$\nabla[\operatorname{Re} f(z)] = \overline{f'(z)}.$$

In particular, if a, b and d are any real numbers,

$$u(z) = d \log|z| \quad \Longrightarrow \quad \nabla u(z) = d/\bar{z}$$

---

[1]The probabilistic interpretation of a streamline is as follows. Diffusion is governed by the heat equation $u_t = \Delta u$, and a harmonic function u corresponds to a steady state satisfying the Laplace equation $\Delta u = 0$. A streamline is a curve across which there is no net diffusion in this steady state. If we think of the diffusion process as resulting from particles moving along Brownian paths, this means that the rate of particles crossing from left to right at each point along the streamline equals the rate crossing from right to left.
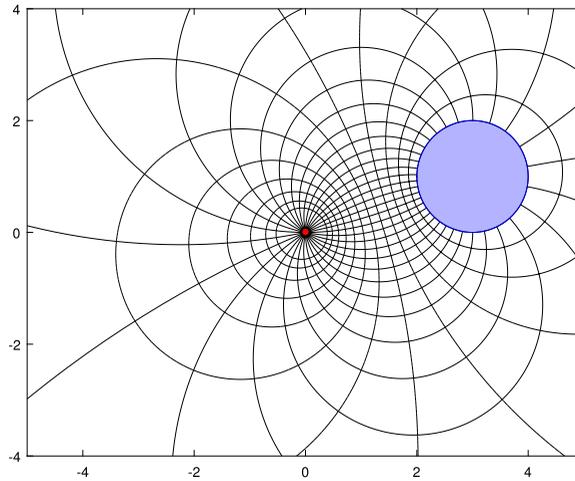
FIGURE 2. Repetition of Figure 1 but now with an orthogonal system of curves also included (streamlines), computed with `disk1ode` by solving the ODE (2.3).

and

$$u(z) = a \operatorname{Re} (z^{-k}) + b \operatorname{Im} (z^{-k}) \quad \implies \quad \nabla u(z) = -k(a + bi)/\bar{z}^{k+1}.$$

Our code for climbing the gradients of Figure 1 is called `disk1ode`, and the results are shown in Figure 2. ODE methods for tracking contours have been used by Gautschi and Waldvogel, as presented in [27, Ch. 25], by Weideman (for climbing poles of solutions of Painlevé equations, unpublished), and no doubt by others.

Careful readers may note that to solve the ODE (2.3) numerically, the codes in the Appendix call Matlab `ode23` rather than, as one might expect, `ode45`. Both choices work well for regions bounded by disks, but in the case of slits, we find that `ode45`, with its larger time steps, more often introduces anomalies as a contour approaches a slit because of hopping over the slit and making erroneous choices of branch.

3 Green function for several disks

Our next example is the same as before, except that instead of one disk defined by $|z - c| = r$, we have J disks defined by $|z - c_j| = r_j$, $1 \le j \le J$. The series approximation is a generalization of (2.2),

$$u(z) = \log |z| + C + \sum_{j=1}^{J} \left\{ d_j \log |z - c_j| + \sum_{k=1}^{N} [a_{jk} \operatorname{Re}((z - c_j)^{-k}) + b_{jk} \operatorname{Im} ((z - c_j)^{-k})] \right\},$$

(3.1)

together with the condition
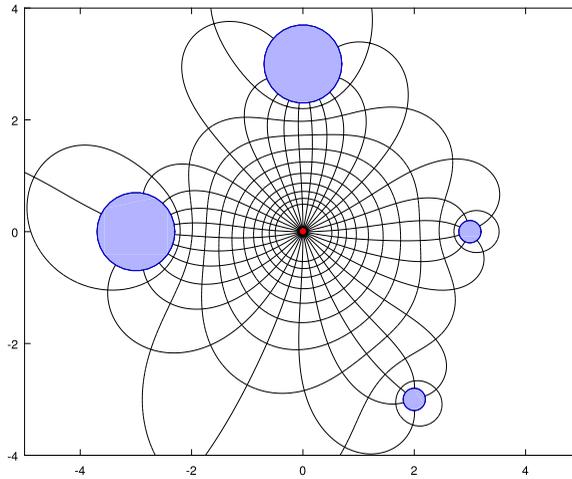
$$\sum_{j=1}^{J} d_j = -1.$$

(3.2)

FIGURE 3. An analogous computation with several disks (code `disks`). Note that even very small disks may have a large influence on the solution.

The only new issue that arises in moving from (2.2) to (3.1) is that the coefficients d_j are now unknowns, which are determined by imposing the condition (3.2) to ensure nonsingular behaviour at $z = \infty$. We do this by appending one more row to the matrix A and one more entry to the right-hand side vector, though one could equally well remove one of the variables such as d_1. The code is called `disks`.

Figure 3 shows the equipotentials and streamlines for a configuration with four disks, two large and two small. It is interesting to record the coefficients $d_1, \ldots, d_4$, which are the negatives of the harmonic measures of each disk:

$$d_1 = -0.342977, \quad d_2 = -0.315902, \quad d_3 = -0.182248, \quad d_4 = -0.158873.$$

The disks are numbered in clockwise order beginning with the big one on the left, and the diminishing sizes of these coefficients correspond to the diminishing proportions of streamlines hitting each disk. (We list the numbers to six digits, although with $N = 10$ they have already converged to 13 digits of accuracy.) Note that although the small disks are much smaller than the big ones, their harmonic measures are only somewhat smaller. This is a familiar effect in potential theory, or equivalently in probability theory: the influence of a structure of radius r diminishes only at a rate $O(1/\log r)$ as $r \to 0$. See [9, 48], and the Cantor set example of Section 5.

Figure 4 shows the result of a variant computation. Here, instead of $u(z) = 0$ as the boundary condition on all four disks, we require $u(z) = 0$ on the two larger disks and $u(z) = -1$ on the two smaller ones (a straightforward change in the least-squares problem, not listed in the Appendix). The equipotentials and streamlines change considerably, and the numbers d_j take quite different values:

$$d_1 = -0.493167, \quad d_2 = -0.492543, \quad d_3 = -0.006514, \quad d_4 = -0.007775.$$
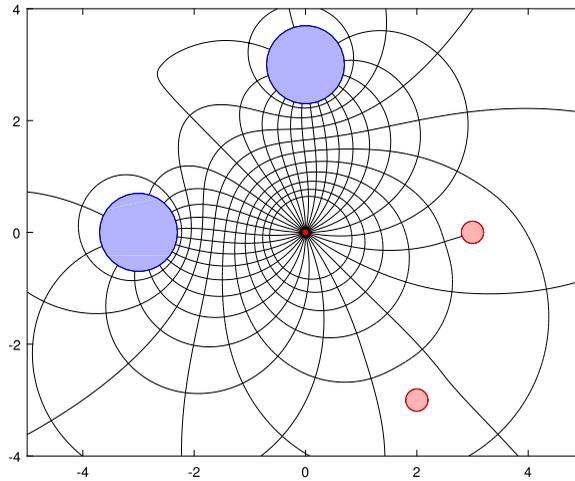
FIGURE 4. Modification in which the two small disks take boundary values $u = -1$ rather than $u = 0$. This diminishes their influence greatly.

The tiny values of d_3 and d_4 show that the small disks now have little influence on the solution. This is because the values of u specified on their boundaries are not much different from the values u would have taken in their absence.[1]

4 Green function for one or several slits

If c and $r \neq 0$ are complex numbers, then $c + r[-1, 1]$ is a complex interval that we call a *slit*, and the exterior of the unit disk in the w-plane is conformally mapped to the exterior of the slit by the function

$$z = c + r(w + w^{-1})/2.$$

The inverse map can be written for $z \notin c + r[-1, 1]$ by

$$w = z_c + s(z_c) \sqrt{z_c^2 - 1}, \quad z_c = (z - c)/r, \tag{4.1}$$

where $s(z_c)$ takes the value $+1$ for z_c in the open right half-plane or the positive imaginary axis and -1 for z_c in the open left half-plane or the negative imaginary axis. (These choices are designed to work with the standard branch of the square root.) For $z \in c + r[-1, 1]$, that is, $z_c \in [-1, 1]$, there are two values of w, and we avoid evaluating $w(z)$ for such values.

By transplanting the powers w^{-k}, these maps give us good bases for series expansions in regions with slits. Equation (2.2) becomes

$$u(z) = \log |z| - \log |w| + C + \sum_{k=1}^{N} [a_k \operatorname{Re}(w^{-k}) + b_k \operatorname{Im}(w^{-k})],$$

---

[1] Bengt Fornberg points out in an email: "If you put $u(z) = +1$ rather than -1 on them, in spite of being small, they would put up a massive field barrier. I guess this is the idea behind the old vacuum tube".
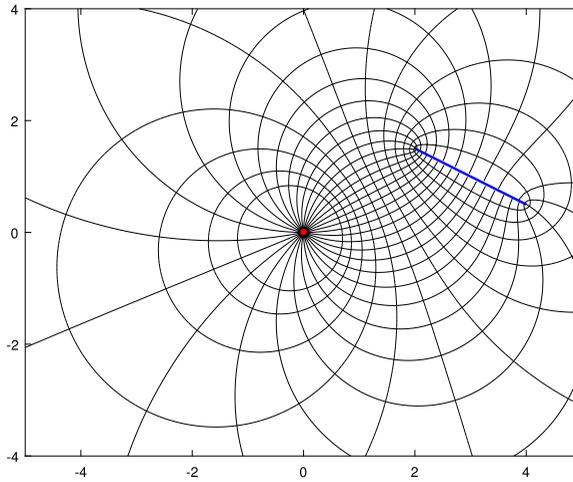
FIGURE 5. Green function $u(z)$ outside a slit computed with `slit1`. The same method is used as in Figure 1, except with basis functions transplanted from the exterior of a disk to the exterior of the slit. Computing the difference in imaginary part from one end of the slit to the other along each side (or equivalently, integrating the gradient) shows that 58.2625% of the harmonic measure falls on the side facing the origin.

and the code `slit1` is an analogue of `disk1`. Figure 5 shows the plot produced by this code, which uses the choices $c = 3 + i$, $r = 1 - 0.5i$.

To treat a region with several slits, we can use this analogue of (3.1),

$$u(z) = \log|z| + C + \sum_{j=1}^{J} \left\{ d_j \log|w_j(z)| + \sum_{k=1}^{N} [a_{jk} \operatorname{Re}(w_j(z)^{-k}) + b_{jk} \operatorname{Im}(w_j(z)^{-k})] \right\},$$

where $w_j(z)$ denotes the map (4.1) with parameters c_j and r_j. Without further discussion, we present in Figure 6 the result of executing `slits`.

5 Approximations to the Cantor set

The Cantor set is a canonical example of a fractal, a subset of the real axis with infinitely many pieces, zero length and nonzero capacity. Figure 7 illustrates that Green functions for finite approximations to a Cantor set are readily computed by series expansions. The plots show that the potential fields associated with coarse approximations to the Cantor set quickly settle down to close to the limiting form, a consequence of the "familiar effect" mentioned in the penultimate paragraph of Section 3. Figure 8 further illustrates this with closeups for $m = 5$ and $m = 6$.

Starting with the interval $[-1.5, 1.5]$ of length 3, these domains are constructed by removing the middle third of each remaining piece m times, where m is a positive integer. To compute the fields of Figure 7, we could have used the code `slits` as written, but there are many symmetries to be taken advantage of. Because of the real
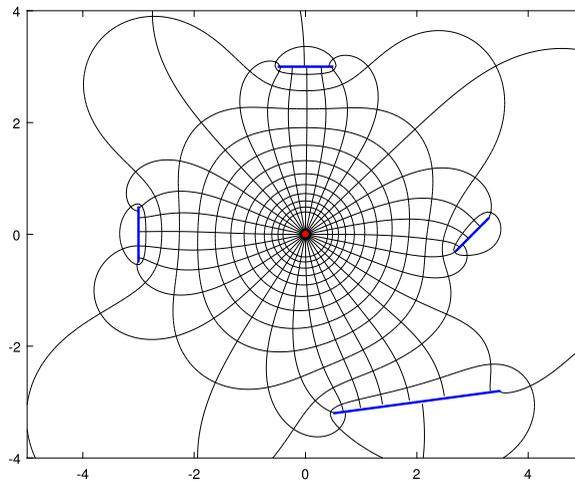
FIGURE 6. Green function $u(z)$ outside several slits, computed with `slits`.

symmetry, the imaginary terms can be removed from the expansions; also it is only necessary to sample on one side of each slit. Because of the even symmetry, one can combine terms in pairs from the left and right half-planes, and use sample points only in one of the half-planes. And, of course, since the solution computed is left-right and top-down symmetric, one need only compute field lines in a quadrant. A further benefit is that for $m \geq 3$, the slits are so short and well separated that a small value of N suffices for six-digit accuracy or more; we take $N = \max\{2, 6 - m\}$. The code `cantor` used for Figure 7 exploits these effects, and for plots with $m = 4, 5, \ldots, 10$, the times required on a 2016 laptop are about 0.2, 0.3, 0.4, 0.8, 2.4, 12 and 80 s, respectively. These geometries have $32, 64, \ldots, 2048$ slits.

The negatives of the coefficients d_j of the calculation give us the harmonic measures of each slit. From inside out, here are the harmonic measures of the 2^{m-1} slits in the right half-plane for the level m finite Cantor sets with $m = 1, 2, 3, 4$. All these figures are believed to be accurate to the six digits listed:

$m = 1$: 1/2
$m = 2$: 0.367776, 0.132224
$m = 3$: 0.253289, 0.111676, 0.066706, 0.068329
$m = 4$: 0.162063, 0.088794, 0.058116, 0.054538, 0.038156, 0.029363, 0.029460, 0.039509.

Analysis of such numbers confirms that once the slits in a finite Cantor set are small, not much changes except very close to the slits. For example, suppose one adds up the first halves of the harmonic measures as listed above to determine the total harmonic measure of the half of the slits closer to the origin. For $m = 4, 5, \ldots, 10$ one finds that the measures add up to about 0.367776, 0.364965, 0.363512, 0.362773, 0.362397, 0.362205, 0.362107. These sums converge to a limit of about 0.362007. Doubling
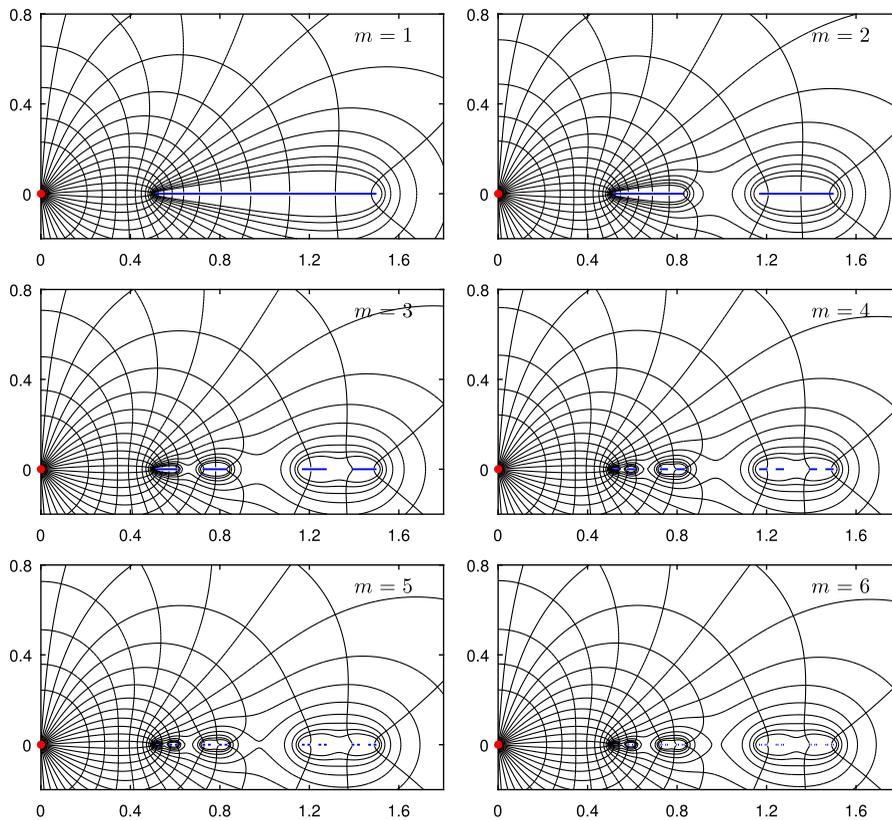
FIGURE 7. Green function $u(z)$ for finite approximations to the Cantor set with 2^m slits, $m = 1, \ldots, 6$, computed with `cantor`. The solution is left-right and up-down symmetric, so only a portion of the right half-plane is shown. Because of the $O(1/\log r)$ effect associated with structures of size $r \ll 1$, the field lines quickly settle down to nearly their final form. The computation of these six images takes a total of about 2 s on a 2016 laptop.

FIGURE 8. Closeups of the last two images of Figure 7.

this figure to account for the left half-plane, we see that the inner slits of a Cantor set correspond to about 72.4% of the harmonic measure.

Other numerical computations related to the Cantor set can be found in [30, 39, 49].

6 Other Laplace problems

The examples we have shown all involve an unbounded domain, a logarithmic singularity, boundaries consisting of circles or slits, and constant Dirichlet boundary condi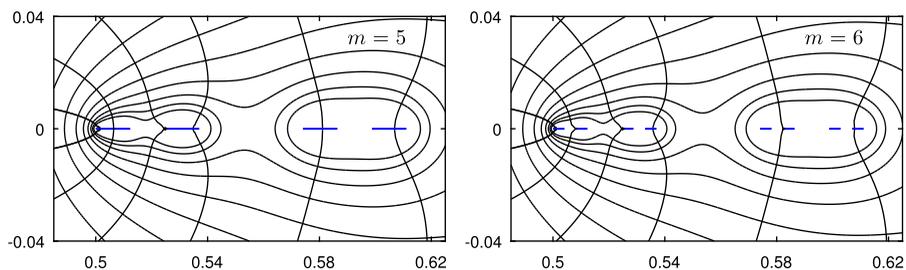tions on each boundary component. We now indicate how series methods can be applied for problems without these features.

Nonconstant boundary conditions. Here it is simply a matter of sampling the boundary condition in an obvious fashion. If the boundary condition and the boundary itself are smooth, one can expect rapid convergence.

Neumann or Robin boundary conditions. Boundary conditions involving derivatives of the function u can be handled in the same manner as Dirichlet conditions: differentiate the series representation and include the conditions in the least-squares problem. An example called `rayleigh_disks` is given in [55].

Bounded domains. The presence of an outer boundary makes it necessary to include positive-degree terms in a series expansion. For example, suppose we have a Laplace problem in an annulus $r_1 < |z| < r_2$ with boundary data prescribed on the inner and outer circles. Here we would need a series involving the real parts of both positive and negative (and zero) powers of z, as well as $\log(z)$. Note that this is analogous to the Laurent series appropriate for an analytic function in an annulus, except for the inclusion of the $\log(z)$ term, which is not relevant to analytic functions since its imaginary part is not single-valued.

More general boundary shapes. Smooth boundary components can be treated by the same methods we have demonstrated. For a nonsmooth boundary component that is not simply a slit, one must expect slow convergence unless special steps are taken. One approach is to include additional terms capturing the local behaviour of singularities at corners, as is explored for the Helmholtz rather than Laplace equation in [6, 7, 25]. The important point to note in series methods is that singularities need only be approximated locally; the boundary matching will take care of the global connections. This is in contrast to methods based on conformal mapping, which require one to resolve global relationships of singularities before progress is made on the Laplace problem.

Figure 9, produced by the code `bounded`, illustrates the solution of a Laplace problem in a bounded domain with no log singularities. The weights d_2 and d_3 on the terms $\log|z - z_2|$ and $\log|z - z_3|$ come out as -0.840513 and -0.450685.

7 Mathematical foundations and history

The ideas underlying series expansion methods date to Runge's theorem of 1885 [52].[1] Runge showed that if f is an analytic function on a simply connected compact set K in the complex plane, it can be approximated arbitrarily closely on K

---

[1]Runge is a hero of mine, who moved from pure to applied mathematics during his career and late in life was appointed at Göttingen effectively as one of the first professors of numerical analysis in the world. He was born 99 years before me to the day.
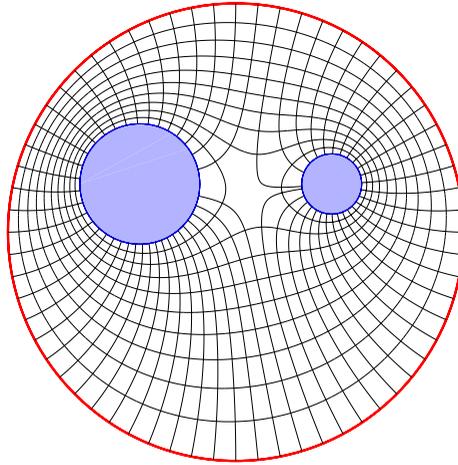
FIGURE 9. Solution of a Laplace problem in a bounded region. The boundary conditions are $u = 0$ on the outer circle and $u = 1$ on the inner ones.

by polynomials. More generally, if K is multiply connected, say with J holes, then f can be approximated on K by rational functions with poles at arbitrarily prescribed points in each of the holes. Here is how the theorem is stated by Gaier [26], with K^C denoting the complement of K in the complex plane $\mathbb{C}$.

Theorem 2 (Runge 1885). *Suppose K is compact in $\mathbb{C}$ and f is analytic on K; further, let $\varepsilon > 0$. Then there exists a rational function R with poles in K^C such that*

$$|f(z) - R(z)| < \varepsilon \quad (z \in K).$$

In general these polynomial and rational approximations cannot come from convergent series, such as Taylor polynomials, but must have coefficients that vary with the degree N. It is enough for the poles of R to be restricted to lie in a fixed set of arbitrarily chosen points $c_1, \ldots, c_J$, one in each hole.

Our concern here has been harmonic functions rather than analytic ones. The two settings are almost the same, since the real part of an analytic function is harmonic, and conversely, a harmonic function u has a harmonic conjugate v such that $u + iv$ is analytic. The complication is that in a multiply connected domain, the function v will in general be multiple-valued, taking different values along different paths around the holes (or equivalently, single-valued on a Riemann surface). This situation is pinned down in the following statement from a beautiful paper by Sheldon Axler called "Harmonic functions from a complex analysis viewpoint" [2]:

LOGARITHMIC CONJUGATION THEOREM. *Suppose Ω is a finitely connected region, with $K_1, \ldots, K_N$ denoting the bounded components of the complement of Ω. For each j, let a_j be a point in K_j. If u is a real valued harmonic function on Ω, then there exist an analytic function f on Ω and real numbers $c_1, \ldots, c_N$ such that*

$$u(z) = Re f(z) + c_1 \log|z - a_1| + \cdots + c_N \log|z - a_N|$$

for every z in Ω.

This theorem leads to the generalization of Runge's theorem from analytic to harmonic functions, which consists essentially of adding a logarithmic term $d_j \log |z - c_j|$ corresponding to each hole, exactly as in our codes. This was first spelled out in a paper by Walsh in 1929 [57] (which Axler describes as "the only place I have been able to find the logarithmic conjugation theorem written down with a proof"). For a more modern (and purer) treatment see the book by Fisher [24, Theorem 2.1 of Ch. 4].

Thus the foundations of series methods for Laplace problems are a century old. It is curious that it is so difficult to find mention of these foundations in the literature of these methods. What happened over the years is that the mathematicians moved on to ever more refined theorems, always seeking the weakest possible regularity assumptions (and rarely mentioning harmonic functions). Building on work by Keldysh in the late 1930s, a landmark of such developments was Mergelyan's theorem of 1951, which allows f to be just continuous on K and analytic in its complex interior, if any, rather than analytic on all of K [26]. Such results are important, but they are quite technical, and remote from most applications.

Walsh and his student Curtiss had an interest in the idea of constructing harmonic approximations based on boundary fitting, though they did not do computations [19]. Unfortunately, like many authors, they focussed on interpolation rather than least-squares. Interpolation formulations, with their square matrices, bring serious challenges of distribution of points and convergence. (Curtiss writes: "The all-important issue in the practical applications will certainly be the correct choice of the interpolation points on the boundary of the region".) When we switch to least-squares, the matrices become rectangular and such difficulties go away so long as one samples in sufficiently many points. Possibly the first advocate of using least-squares for boundary-matching with Laplace problems was Moler in a Stanford technical report of 1969 [41] (see also [21]).

Meanwhile, with little influence from the literature of theoretical mathematics, series expansions were being used in innumerable applications. An early example was Lord Rayleigh, in 1892, who used series to solve Laplace problems in a plane with a periodic array of circular holes removed [50]; a related method for an electromagnetic problem was applied by Záviška in 1913 [58]. The Soviet Union in the mid-20th century was a centre of great expertise in the solution of boundary value problems for linear partial differential equations (PDEs), with leading names including Gakhov, Kantorovich, Krylov, Mikhlin and Mushkelishvili. In 1936 Kantorovich and Krylov published their monograph *Methods for the Approximate Solution of Partial Differential Equations,* which evolved into *Approximate Methods of Higher Analysis,* the latest edition in 1960 [36]. Though the style is not very computational by modern standards, the book has a great deal of material about series expansions for PDEs.

In the computer era, series methods have been applied not only for the Laplace equation but also for the Helmholtz [4, 6, 7], biharmonic [8, 46] and Maxwell equations, among others, and this is the basis for methods with names including Trefftz's method, the method of particular solutions [5–7, 25, 34], point-matching,

the method of plane waves and the method of fundamental solutions [4, 37, 38, 45], also known as the charge simulation method [1, 40, 54]. Concerning the Laplace equation, papers making use of series methods include [9], [17], [20, Section 4] and [23]. These stem from my own methods reported in [55], but there are undoubtedly other unrelated publications. One such that I am aware of is the very nice paper by Rostand [51], which also applies least-squares fitting on the boundary.

Series methods have much the same flavour as the numerical solution of integral equations [44], a very large subject—though they are not the same, as explained in [3]. Integral equations methods tend to take over when the problems feature complicated geometries or nonsmooth data. For sufficiently complex problems, one finds oneself in the worlds of $\mathcal{H}$-matrices and the fast multipole method, which enable extremely complicated geometries to be treated with nearly linear complexity [31–33, 42]. The starting point of the fast multipole method is a recursive use of just the kinds of series we have described. Although the present paper deals with two-dimensional problems, all these methods apply in three dimensions too [10].

8 Numerical considerations

The aim of this paper has been to present series methods, not analyze them. The starting point for analysis will be complex or harmonic approximation theory of the kind mentioned in the last section. Without going into any details, we mention some issues that must arise in a deeper treatment of series methods.

Boundary resolution. The great convenience of a least-squares formulation is that it permits one to put plenty of points along the boundary, thereby bypassing subtle questions related to interpolation. But how big must the ratio npts$/N$ be to achieve satisfactory accuracy? And can this come with guarantees? A mathematical analysis will require attention to matters of polynomial or trigonometric interpolation related to the Runge phenomenon [53] and the study of Lebesgue constants, and sharp answers will depend on regions of analyticity of the solutions being computed [4, 56].

Convergence rate. As $N \to \infty$, the convergence will normally be exponential, at a rate $O(\rho^{-N})$ for some $\rho > 1$, if the boundaries and the boundary data are analytic. The value of ρ will depend on matters of analytic continuation, as above [4]. Only in simple cases would one expect to analyze such rates analytically.

Scaling. We have used powers $(z - c)^{-k}$ for all disks, regardless of their radius. In problems with widely varying scales, however, it may be advantageous to scale such terms relative to the radius. This is related to column scaling of the matrix A.

Complexity. Series methods rely on solving least-squares matrix problems, and the cubic complexity will eventually show up if problems with enough components are considered. In such cases one may turn to hierarchical approaches such as the fast multipole method. As a rule of thumb, it seems clear that one should do this (in two dimensions) for problems with thousands of components, but perhaps not if there are merely hundreds of components.

Nearly touching boundary components. In some problems two holes, say, may nearly touch, and convergence of a series method will degrade. In simple cases one may solve the problem by using a point other than the centre for a local expansion (or relatedly, a local Möbius transformation). In more complicated problems, this is one of the situations where hierarchical methods prove their power [11, 12, 18, 33].

Three dimensions. Nothing that we have done is restricted to two dimensions, apart from the use of a complex variable for convenience [10]. In three dimensions, nevertheless, there is no denying that computations tend to require more human and computer effort, and the role of simple series methods is perhaps smaller than in two dimensions.

Maximum principle. One of the attractions about boundary matching for elliptic problems is that the maximum principle allows easy a posteriori analysis of accuracy. So long as the boundary data are closely matched, as can be verified by sampling finely, one can be assured that the computed solution is accurate. See for example [25, 41].

9 Conclusion

The elementary solution methods we have presented are not always familiar to those who might find them useful. They tend to be eclipsed by more general, more powerful tools, which are necessary for sufficiently complicated problems but rely on much more machinery. An explanation for this situation may lie in the disparate rates of development of mathematics, algorithms, computers and software. Fifty years ago, thanks to Runge and Walsh and Keldysh and others, the mathematical basis of series methods was already in place and known (if not in mathematical detail) to the early computer-era numerical analysts. And so one finds Hockney, for example, publishing a paper in 1964 about series expansions for a Laplace problem involving "a round hole in a square peg" [35]. But it took time for computers to grow powerful enough, and software convenient enough, to enable such methods to be so easily used as we have demonstrated. By the time that had happened, researchers had come to focus on more advanced tools.

As our Cantor set example shows, elementary methods can work well even for regions with hundreds of holes.

Acknowledgements

Appendix

MATLAB codes

```
function disk1   % Green function exterior to a disk, equipotential curves only
%
% We seek the function u(z) that is zero for |z-c| = r and harmonic outside this
% circle, including at z=infty, except with u(z)~log|z| as z->0.  u is expanded as
%
%   u(z) = log|z| - log|z-c| + a(1)
%              + SUM_{k=1}^N a(2k)*real((z-c)^(-k)) + a(2k+1)*imag((z-c)^(-k)) .

c = 3+1i; r = 1;                        % center and radius of disk
N = 10; npts = 3*N;                     % no. expansion terms and sample pts
z = c + r*exp(2i*pi*(1:npts)'/npts);    % sample points
rhs = -log(abs(z)) + log(abs(z-c));     % right-hand side
A = ones(npts,2*N+1);
for k = 1:N                             % set up least-squares matrix
   A(:,2*k  ) = real((z-c).^-k);
   A(:,2*k+1) = imag((z-c).^-k);
end
a = A\rhs;                              % solve least-squares problem

% Contour plot
x = linspace(-5,5,145); y = linspace(-4,4,115); [xx,yy] = meshgrid(x,y);
zz = xx+1i*yy; uu = disk1fun(zz); z = c + r*exp(pi*1i*(-50:50)'/50);
fill(real(z),imag(z),[.7 .7 1]), hold on
plot(z,'b'), plot(0,0,'.r','markersize',13)
levels = -3:.25:-.25; contour(xx,yy,uu,levels,'k'), axis equal, axis([-5 5 -4 4])
set(gca,'xtick',-4:2:4,'ytick',-4:2:4,'fontsize',8), hold off, print -depsc disk1

function u = disk1fun(z)
u = log(abs(z)) - log(abs(z-c)) + a(1);
for k = 1:N, u = u + a(2*k)*real((z-c).^(-k)) +a(2*k+1)*imag((z-c).^(-k)); end
u(abs(z-c)<=r) = NaN;
end

end


function disk1ode   % Green function exterior to a disk
%
% We seek the function u(z) that is zero for |z-c| = r and harmonic outside
% this circle, including at z=infty, except with u(z)~log|z| as z->0.
% u is expanded as
%
%   u(z) = log|z| - log|z-c| + a(1)
%              + SUM_{k=1}^N a(2k)*real((z-c)^(-k)) + a(2k+1)*imag((z-c)^(-k)) .

c = 3+1i; r = 1;                        % center and radius of disk
N = 10; npts = 3*N;                     % no. expansion terms and sample pts
z = c + r*exp(2i*pi*(1:npts)'/npts);    % sample points
rhs = -log(abs(z)) + log(abs(z-c));     % right-hand side
A = ones(npts,2*N+1);
for k = 1:N                             % set up least-squares matrix
   A(:,2*k  ) = real((z-c).^-k);
   A(:,2*k+1) = imag((z-c).^-k);
end
a = A\rhs;                              % solve least-squares problem
```

```
% Contour plot
x = linspace(-5,5,145); y = linspace(-4,4,115); [xx,yy] = meshgrid(x,y); zz = xx+1i*yy;
uu = disk1fun(zz); z = c + r*exp(pi*1i*(-50:50)'/50); fill(real(z),imag(z),[.7 .7 1])
hold on, plot(z,'b'), plot(0,0,'.r','markersize',6), levels = -3:.25:-.25;
contour(xx,yy,uu,levels,'k'), axis equal, axis([-5 5 -4 4])
set(gca,'xtick',-4:2:4,'ytick',-4:2:4,'fontsize',8), op = odeset('events',@event);
for t = pi*(1:32)/16, z0 = .01*exp(1i*t); sol = ode45(@dzdt,[0 500],z0,op);
plot(deval(sol,linspace(0,max(sol.x),300)),'k'), end
plot(0,0,'.r','markersize',13), hold off, print -depsc disk1ode

function u = disk1fun(z)
u = log(abs(z)) - log(abs(z-c)) + a(1);
for k = 1:N, u = u + a(2*k)*real((z-c).^(-k)) + a(2*k+1)*imag((z-c).^(-k)); end
u(abs(z-c)<=r) = NaN;
end

function g = dzdt(t,z)
g = 1./conj(z) - 1./conj(z-c);
for k = 1:N, g = g - k*(a(2*k)+1i*a(2*k+1))./conj(z-c).^(k+1); end
g = g./abs(g);
end

function [val,isterm,dir] = event(t,z)
dir = 0; isterm = 1; val = abs(z-c)-r;
end

end


function disks    % Green function exterior to several disks
%
% We seek the function u(z) that is zero for |z-c(j)| = r(j), j = 1,...,J,
% and harmonic outside these circles, including at z=infty, except with
% u(z)~log|z| as z->0.  u is expanded as
%
%   u(z) = log|z| + C + SUM_{j=1}^J {d(j)*log|z-c(j)|
%           + SUM_{k=1}^N [a(j,k)*real((z-z(j))^-k) + b(j,k)*imag((z-z(j))^-k)]}
%
% with SUM d(j) = -1; all these coefficients are collected in the vector X.
% The unknowns determined by linear least-squares are C, d(1),...,d(J),
% {a(j,k)}, {b(j,k)}.  A has dimensions 1+J*npts by 1+J*(2N+1).

c = [-3 3i 3 2-3i];                    % centers
r = [.7 .7 .2 .2]; J = 4;              % radii
N = 10; npts = 3*N;                    % no. expansion terms and sample pts
circ = exp(2i*pi*(1:npts)'/npts);      % roots of unity
z = []; for j = 1:J
   z = [z; c(j)+r(j)*circ]; end        % sample points on the bndry
A = ones(size(z));                     % constant term
for j = 1:J
   A = [A log(abs(z-c(j)))];           % logarithmic terms
   for k = 1:N                         % set up least-squares matrix
      zck = (z-c(j)).^(-k);
      A = [A real(zck) imag(zck)];     % algebraic terms
   end
end
A = [A; zeros(1,1+J*(2*N+1))];
A(end,2:(2*N+1):end) = 1;
```

```
rhs = [-log(abs(z)); -1];
X = A\rhs;                              % solve least-squares problem
C = X(1); X(1) = [];                    % extract results
d = X(1:2*N+1:end), X(1:2*N+1:end) = [];
a = X(1:2:end); b = X(2:2:end);

% Contour plot
x = linspace(-5,5,145); y = linspace(-4,4,115); [xx,yy] = meshgrid(x,y); zz = xx+1i*yy;
uu = disksfun(zz); z = exp(2i*pi*(0:30)'/30);
for j = 1:J, disk = c(j)+r(j)*z; fill(real(disk),imag(disk),[.7 .7 1])
hold on, plot(disk,'b'), end, levels = -1.9:.2:-.1;
contour(xx,yy,uu,levels,'k'), axis equal, axis([-5 5 -4 4])
set(gca,'xtick',-4:2:4,'ytick',-4:2:4,'fontsize',8), op = odeset('events',@disksevent);
for t = pi*(1:32)/16, z0 = .01*exp(1i*t); sol = ode45(@dzdt,[0 100],z0,op);
plot(deval(sol,linspace(0,max(sol.x),300)),'k'), end
plot(0,0,'.r','markersize',13), hold off, print -depsc disks

function u = disksfun(z)
u = log(abs(z)) + C;
for j = 1:J
  cj = c(j); u = u + d(j)*log(abs(z-cj));
  for k = 1:N, zck = (z-cj).^(-k); kk = k+(j-1)*N;
    u = u+a(kk)*real(zck)+b(kk)*imag(zck);
  end
  u(abs(z-cj)<=r(j)) = NaN;
end
end

function g = dzdt(t,z)
g = conj(1./z);
for j = 1:J
  zcj = z - c(j); g = g + d(j)./conj(zcj);
  for k = 1:N, kk = k+(j-1)*N;
    g = g - k*(a(kk)+1i*b(kk))./conj(zcj).^(k+1);
  end
end
g = g./abs(g);
end

function [val,isterm,dir] = disksevent(t,z)
dir = zeros(J,1); isterm = ones(J,1); val = abs(z-c.')-r.';
end

end


function slit1   % Green function exterior to a slit
%
% We seek the function u(z) that is zero on the interval c + r[-1,1] and harmonic outside
% this slit, including at z=infty, except with u(z)~log|z| as z->0.  u is expanded as
%
%   u(z) = log|z| - log|w| + a(1)
%               + SUM_{k=1}^N a(2k)*real(w^(-k)) + a(2k+1)*imag(w^(-k))
%
% where w(z) is a Joukowski map of exterior(slit) to exterior(unit disk).

c = 3+1i; r = 1-.5i;                    % center and half-length of slit
N = 10; npts = 3*N;                     % no. expansion terms and sample pts
circ = (1+1e-12)*exp(2i*pi*(1:npts)'/npts);
```

```
z = c + r*(circ+1./circ)/2;                % sample points
w = wz(z); rhs = -log(abs(z)) + log(abs(w));  % right-hand side
A = ones(npts,2*N+1);
for k = 1:N                                % set up least-squares matrix
   A(:,2*k  ) = real(w.^-k);
   A(:,2*k+1) = imag(w.^-k);
end
a = A\rhs;                                 % solve least-squares problem

% Contour plot
x = linspace(-5,5,145); y = linspace(-4,4,115); [xx,yy] = meshgrid(x,y);
zz = xx+1i*yy; uu = slit1fun(zz); z = c + r*[-1 1];
plot(z,'b','linewidth',1.4), hold on
levels = -3:.25:-.25; contour(xx,yy,uu,levels,'k'), axis equal, axis([-5 5 -4 4])
set(gca,'xtick',-4:2:4,'ytick',-4:2:4,'fontsize',8)
op = odeset('events',@event);
for t = pi*(1:32)/16, z0 = .01*exp(1i*t); sol = ode23(@dzdt,[0 50],z0,op);
plot(deval(sol,linspace(0,max(sol.x),300)),'k'), end
plot(0,0,'.r','markersize',13), hold off, print -depsc slit1

function u = slit1fun(z)
w = wz(z); u = log(abs(z)) - log(abs(w)) + a(1);
for k = 1:N, u = u + a(2*k)*real(w.^(-k)) + a(2*k+1)*imag(w.^(-k)); end
end

function w = wz(z)
zc = (z-c)/r; sgn = real(zc)>0|(real(zc)==0&imag(zc)>0); sgn = 2*sgn - 1;
w = zc + sgn.*sqrt(zc.^2-1);
end

function g = dzdt(t,z)
zc = (z-c)/r; sgn = real(zc)>0|(real(zc)==0&imag(zc)>0); sgn = 2*sgn - 1;
cw = conj(zc+sgn.*sqrt(zc.^2-1)); dwdzc = conj((1+sgn*zc./sqrt(zc.^2-1))/r);
g = 1./conj(z) - dwdzc./cw;
for k = 1:N, g = g - k*(a(2*k)+1i*a(2*k+1))*dwdzc./cw.^(k+1); end
g = g./abs(g);
end

function [val,isterm,dir] = event(t,z)
dir = 0; isterm = 1; val = abs(wz(z))-1.03;
end

end


function slits   % Green function exterior to several slits
%
% We seek the function u(z) that is zero on the complex intervals c(j)+r(j)[-1,1]
% j = 1,...,J, and harmonic outside these slits, including at z=infty, except with
% u(z)~log|z| as z->0.  u is expanded as
%
%   u(z) = log|z| + C + SUM_{j=1}^J {d(j)*log|wj(z)|
%           + SUM_{k=1}^N [a(j,k)*real(wj(z)^(-k)) + b(j,k)*imag(wj(z)^(-k))]},
%
% where wj(z) is a Joukowski map of exterior(slit j) to exterior(unit disk),
% with SUM d(j) = -1; all these coefficients are collected in the vector X.
% The unknowns determined by linear least-squares are C, d(1),...,d(J),
% {a(j,k)}, {b(j,k)}.  A has dimensions 1+J*npts by 1+J*(2N+1).
```

```
c = [-3 3i 3 2-3i];                       % centers
r = [.5i .5 .3+.3i 1.5+.2i]; J = 4;       % radii
N = 10; npts = 3*N;                       % no. expansion terms and sample pts
circ = (1+1e-8)*exp(2i*pi*(1:npts)'/npts); % roots of unity
z = []; for j = 1:J
   z = [z; c(j)+r(j)*(circ+1./circ)/2]; end % sample points on the bndry
A = ones(size(z));                        % constant term
for j = 1:J
   wj = wz(z,j); A = [A log(abs(wj))];     % logarithmic terms
   for k = 1:N                             % set up least-squares matrix
      wck = wj.^(-k);
      A = [A real(wck) imag(wck)];         % algebraic terms
   end
end
A = [A; zeros(1,1+J*(2*N+1))];
A(end,2:(2*N+1):end) = 1;
rhs = [-log(abs(z)); -1];
X = A\rhs;                                % solve least-squares problem
C = X(1); X(1) = [];                      % extract results
d = X(1:2*N+1:end), X(1:2*N+1:end) = [];
a = X(1:2:end); b = X(2:2:end);

% Contour plot
x = linspace(-5,5,145); y = linspace(-4,4,115); [xx,yy] = meshgrid(x,y);
zz = xx+1i*yy; uu = slitsfun(zz);
for j = 1:J, slit = c(j)+r(j)*[-1 1]; plot(slit+1e-12i,'b','linewidth',1.4), hold on, end
levels = -2.3:.2:-.1; contour(xx,yy,uu,levels,'k'), axis equal, axis([-5 5 -4 4])
set(gca,'xtick',-4:2:4,'ytick',-4:2:4,'fontsize',8), op = odeset('events',@event);
for t = pi*(1:32)/16, z0 = .01*exp(1i*t); sol = ode23(@dzdt,[0 100],z0,op);
plot(deval(sol,linspace(0,max(sol.x),300)),'k'), end
plot(0,0,'.r','markersize',13), hold off, print -depsc slits

function u = slitsfun(z)
u = log(abs(z)) + C;
for j = 1:J
   cj = c(j); w = wz(z,j); u = u + d(j)*log(abs(w));
   for k = 1:N, wk = w.^(-k); kk = k+(j-1)*N;
      u = u+a(kk)*real(wk)+b(kk)*imag(wk);
   end
   u(abs(w)<=1.01) = NaN;
end
end

function w = wz(z,j)
zc = (z-c(j))/r(j); sgn = real(zc)>0|(real(zc)==0&imag(zc)>0); sgn = 2*sgn - 1;
w = zc + sgn.*sqrt(zc.^2-1);
end

function g = dzdt(t,z)
g = 1./conj(z);
for j = 1:J
   zc = (z-c(j))/r(j); sgn = real(zc)>0|(real(zc)==0&imag(zc)>0); sgn = 2*sgn - 1;
   cw = conj(zc+sgn.*sqrt(zc.^2-1)); dwdzc = conj((1+sgn*zc./sqrt(zc.^2-1))/r(j));
   g = g + d(j)*dwdzc./cw;
   for k = 1:N, kk = k+(j-1)*N; g = g - k*(a(kk)+1i*b(kk))*dwdzc./cw.^(k+1); end
end
g = g./abs(g);
end
```

```
function [val,isterm,dir] = event(t,z)
dir = zeros(J,1); isterm = ones(J,1);
val = zeros(J,1); for j = 1:J; val(j) = abs(wz(z,j))-1.03; end
end

end


function cantor  % Green function exterior to a finite approximate Cantor set
%
% We seek the function u(z) that is zero on the real intervals c(j)+r(j)[-1,1]
% j = 1,...,J, and harmonic outside these slits, including at z=infty, except with
% u(z)~log|z| as z->0.  u is expanded as
%
%   u(z) = log|z| + C + SUM_{j=1}^J {d(j)*log|wj(z)|
%            + SUM_{k=1}^N a(j,k)*real(wj(z)^(-k)),
%
% where wj(z) is a Joukowski map of exterior(slit j) to exterior(unit disk),
% with SUM d(j) = -1; all these coefficients are collected in the vector X.
% The unknowns determined by linear least-squares are C, d(1),...,d(J),
% {a(j,k)}.  A has dimensions 1+J*npts by 1+J*(N+1).

m = 5; J=2^m; c = 0; r = 1.5;           % level of finite Cantor set
for i = 1:m
  r = r/3; c = [c+2*r c-2*r];
end
N = max(2,6-m); npts = round(1.5*N);    % no. expansion terms and sample pts
circ = (1+1e-12)*exp(1i*pi*(.5:npts)'/npts); % roots of unity
z = []; for j = 1:J
  z = [z; c(j)+r*(circ+1./circ)/2]; end % sample points on the bndry
A = ones(size(z));                      % constant term
for j = 1:J
  wj = wz(z,j); A = [A log(abs(wj))];    % logarithmic terms
  for k = 1:N, A = [A real(wj.^(-k))]; end % set up least-squares matrix
end
A = [A; zeros(1,1+J*(N+1))];
A(end,2:N+1:end) = 1;
rhs = [-log(abs(z)); -1];
X = A\rhs;                              % solve least-squares problem
C = X(1); X(1) = [];                    % extract results
d = X(1:N+1:end); X(1:N+1:end) = []; a = X;

% Contour plot
x = linspace(0,1.8,145); y = linspace(-0.2,0.8,75); [xx,yy] = meshgrid(x,y);
zz = xx+1i*yy; uu = cantorfun(zz);
for j = 1:J, slit = c(j)+r*[-1 1]; plot(slit+1e-12i,'-b','linewidth',1.2), hold on, end
levels = -10.^(-1.2:.1:.2); contour(xx,yy,uu,levels,'k'), axis equal, axis([0 1.8 -.2 .8])
set(gca,'xtick',0:.4:2,'ytick',-.8:.4:.8,'fontsize',5), op = odeset('events',@event);
for t = pi*(1:2:23)/48, z0 = .01*exp(1i*t); sol = ode23(@dzdt,[0 100],z0,op);
z = deval(sol,linspace(0,max(sol.x),300)); plot(z,'k'), plot(conj(z),'k'), end
plot(0,0,'.r','markersize',16), hold off

function u = cantorfun(z)
u = log(abs(z)) + e;
for j = 1:J
  cj = c(j); w = wz(z,j); u = u + d(j)*log(abs(w));
  for k = 1:N, wk = w.^(-k); kk = k+(j-1)*N; u = u+a(kk)*real(wk); end
  u(abs(w)<=1.01) = NaN;
end
```

```
end

function w = wz(z,j)
zc = (z-c(j))/r; sgn = real(zc)>0|(real(zc)==0&imag(zc)>0); sgn = 2*sgn - 1;
w = zc + sgn.*sqrt(zc.^2-1);
end

function g = dzdt(t,z)
g = 1./conj(z);
for j = 1:J
  zc = (z-c(j))/r; sgn = real(zc)>0|(real(zc)==0&imag(zc)>0); sgn = 2*sgn - 1;
  cw = conj(zc+sgn.*sqrt(zc.^2-1)); dwdzc = conj((1+sgn*zc./sqrt(zc.^2-1))/r);
  g = g + d(j)*dwdzc./cw;
  for k = 1:N, kk = k+(j-1)*N; g = g - k*a(kk)*dwdzc./cw.^(k+1); end
end
g = g./abs(g);
end

function [val,isterm,dir] = event(t,z)
dir = zeros(J,1); isterm = ones(J,1);
val = zeros(J,1); for j = 1:J; val(j) = abs(wz(z,j))-(1+.01/r); end
end

end



function bounded   % Harmonic function in a region bounded by disks
%
% We seek the function u with u(z)=0 for |z-c(1)|=r(1)>>1 and u(z)=1 for |z-c(j)|=r(j),
% j = 2,...,J, that is harmonic in the region between these circles.  u is expanded as
%
%   u(z) =  C + SUM_{k=1}^N [a(1,k)*real((z-z(j))^k + b(1,k)*imag((z-z(j))^k]
%              + SUM_{j=2}^J {d(j)*log|z-c(j)|
%              +   SUM_{k=1}^N [a(j,k)*real((z-z(j))^-k + b(j,k)*imag((z-z(j))^-k]}
%
% all these coefficients are collected in the vector X. The unknowns determined by
% linear least-squares are C, d(2),...,d(J), {a(j,k)}, {b(j,k)}.  A has dimensions
% J*npts by J*(2N+1).

c = [0 -1.6+.8i 1.6+.8i];              % centers
r = [3.8 1 .5]; J = 3;                 % radii
N = 10; npts = 3*N;                    % no. expansion terms and sample pts
circ = exp(2i*pi*(1:npts)'/npts);      % roots of unity
z = []; for j = 1:J
  z = [z; c(j)+r(j)*circ]; end         % sample points on the bndry
A = ones(size(z));                     % constant term
for j = 1:J
  s = 1;
  if j>1
    s = -1; A = [A log(abs(z-c(j)))];  % logarithmic terms
  end
  for k = 1:N                          % set up least-squares matrix
    zck = (z-c(j)).^(s*k);
    A = [A real(zck) imag(zck)];       % algebraic terms
  end
end
rhs = ones(size(z)); rhs(1:npts) = 0;
X = A\rhs;                             % solve least-squares problem
C = X(1); X(1) = [];                   % extract results
```

```
d = [NaN; X(2*N+1:2*N+1:end)]
X(2*N+1:2*N+1:end) = [];
a = X(1:2:end); b = X(2:2:end);

% Contour plot
x = linspace(-5,5,145); y = linspace(-4,4,115); [xx,yy] = meshgrid(x,y); zz = xx+1i*yy;
uu = boundedfun(zz); z = exp(2i*pi*(0:300)'/150);
plot(c(1)+r(1)*z,'r','linewidth',1.2), hold on
for j = 2:J, disk = c(j)+r(j)*z; fill(real(disk),imag(disk),[.7 .7 1])
plot(disk,'b'), end, levels = .1:.1:.9;
contour(xx,yy,uu,levels,'k'), axis equal, axis([-5 5 -4 4])
set(gca,'xtick',-4:2:4,'ytick',-4:2:4,'fontsize',8), op = odeset('events',@boundedevent);
for t = pi*(1:64)/32, z0 = r(1)*exp(1i*t); sol = ode23(@dzdt,[0 10],z0,op);
plot(deval(sol,linspace(0,max(sol.x),300)),'k'), end
hold off, axis off, print -depsc bounded

function u = boundedfun(z)
u = C*ones(size(z));
for k = 1:N
   zck = (z-c(1)).^k; u = u+a(k)*real(zck)+b(k)*imag(zck);
end
u(abs(z-c(1))>=r(1)) = NaN;
for j = 2:J
   cj = c(j); u = u + d(j)*log(abs(z-cj));
   for k = 1:N
      zck = (z-cj).^(-k); kk = k+(j-1)*N; u = u+a(kk)*real(zck)+b(kk)*imag(zck);
   end
   u(abs(z-cj)<=r(j)) = NaN;
end
end

function g = dzdt(t,z)
g = zeros(size(z));
for k = 1:N, g = g + k*(a(k)+1i*b(k)).*conj(z-c(1)).^(k-1); end
for j = 2:J
   zcj = z - c(j); g = g + d(j)./conj(zcj);
   for k = 1:N, kk = k+(j-1)*N;
      g = g - k*(a(kk)+1i*b(kk))./conj(zcj).^(k+1);
   end
end
g = g./abs(g);
end

function [val,isterm,dir] = boundedevent(t,z)
dir = zeros(J,1); isterm = ones(J,1); val = abs(z-c.')-r.';
end

end
```

References

[1] K. Amano, D. Okano, H. Ogata and M. Sugihara, "Numerical conformal mappings onto the linear slit domain", *Jpn. J. Ind. Appl. Math.* **29** (2012) 165–186; doi:10.1007/s13160-012-0058-0.

[2] S. Axler, "Harmonic functions from a complex analysis viewpoint", *Amer. Math. Monthly* **93** (1986) 246–258; doi:10.1080/00029890.1986.11971799.

[3] A. P. Austin, P. Kravanja and L. N. Trefethen, "Numerical algorithms based on analytic function values at roots of unity", *SIAM J. Numer. Anal.* **52** (2014) 1795–1821; doi:10.1137/130931035.

[4] A. H. Barnett and T. Betcke, "Stability and convergence of the method of fundamental solutions for Helmholtz problems on analytic domains", *J. Comput. Phys.* **227** (2008) 7003–7026; doi:10.1016/j.jcp.2008.04.008.

[5] S. Bergman, "Functions satisfying certain partial differential equations of elliptic type and their representation", *Duke Math. J.* **14** (1947) 349–366; doi:10.1215/S0012-7094-47-01428-2.

[6] T. Betcke and L. N. Trefethen, "Reviving the method of particular solutions", *SIAM Rev.* **47** (2005) 469–491; doi:10.1137/S0036144503437336.

[7] T. Betcke and L. N. Trefethen, "Computed eigenmodes of planar regions", *Contemp. Math.* **412** (2006) 297–314; http://citeseerx.ist.psu.edu/viewdoc/download?doi=10.1.1.666.5656&rep= rep1&type=pdf.

[8] J. M. Bourot and F. Moreau, "Sur l'utilisation de la série cellulaire pour le calcul d'écoulements plans de Stokes en canal indéfini: application au cas d'un cylindre circulaire en translation", *Mech. Res. Commun.* **14** (1987) 187–197.

[9] S. J. Chapman, D. P. Hewett and L. N. Trefethen, "Mathematics of the Faraday cage", *SIAM Rev.* **57** (2015) 398–417; doi:10.1137/140984452.

[10] H. Cheng, "On the method of images for systems of closely spaced conducting spheres", *SIAM J. Appl. Math.* **61** (2001) 1324–1337; doi:10.1137/S0036139999364992.

[11] H. Cheng and L. Greengard, "On the numerical evaluation of electrostatic fields in dense random dispersions of cylinders", *J. Comput. Phys.* **136** (1997) 629–639; doi:10.1006/jcph.1997.5787.

[12] H. Cheng and L. Greengard, "A method of images for the evaluation of electrostatic fields in systems of closely spaced conductors", *SIAM J. Appl. Math.* **58** (1998) 122–141; doi:10.1137/S0036139996297614.

[13] D. G. Crowdy, "Geometric function theory: a modern view of a classical subject", *Nonlinearity* **21** (2008) T205–T219; doi:10.1088/0951-7715/21/10/T04.

[14] D. G. Crowdy, "Conformal slit maps in applied mathematics", *ANZIAM J.* **53** (2012) 171–189; doi:10.1017/S1446181112000119.

[15] D. G. Crowdy, E. H. Kropf, C. C. Green and M. M. S. Nasser, "The Schottky–Klein prime function: a theoretical and computational tool for applications", *IMA J. Appl. Math.* **81** (2016) 589–628; doi:10.1093/imamat/hxw028.

[16] D. Crowdy and J. Marshall, "Conformal mappings between canonical multiply connected domains", *Comput. Methods Funct. Theory* **6** (2006) 59–76; doi:10.1007/BF03321118.

[17] D. G. Crowdy and J. S. Marshall, "Computing the Schottky–Klein prime function on the Schottky double of planar domains", *Comput. Methods Funct. Theory* **7** (2007) 293–308; doi:10.1007/BF03321646.

[18] D. G. Crowdy, S. Tanveer and T. DeLillo, "Hybrid basis scheme for computing electrostatic fields exterior to close-to-touching disks", *IMA J. Numer. Anal.* **36** (2016) 743–769; doi:10.1093/imanum/drv030.

[19] J. H. Curtiss, "Interpolation by harmonic polynomials", *J. SIAM* **10** (1962) 709–736; doi:10.1137/0110055.

[20] T. K. DeLillo, T. A. Driscoll, A. R. Elcrat and J. A. Pfaltzgraff, "Radial and circular slit maps of unbounded multiply connected circle domains", *Proc. R. Soc. Lond.* A **464** (2008) 1719–1737; doi:10.1098/rspa.2008.0006.

[21] T. K. DeLillo, A. R. Elcrat, E. H. Kropf and J. A. Pfaltzgraff, "Efficient calculation of Schwarz–Christoffel transformations for multiply connected domains using Laurent series", *Comput. Methods Funct. Theory* **13** (2013) 307–336; doi:10.1007/s40315-013-0023-1.

[22] T. A. Driscoll and L. N. Trefethen, *Schwarz–Christoffel mapping* (Cambridge University Press, Cambridge, 2002).

[23] M. D. Finn, S. M. Cox and H. M. Byrne, "Topological chaos in inviscid and viscous mixers", *J. Fluid Mech.* **493** (2003) 345–361; doi:10.1017/S0022112003005858.

[24] S. D. Fisher, *Function theory on planar domains: a second course in complex analysis* (Dover Publ., New York, 2007).

[25] L. Fox, P. Henrici and C. Moler, "Approximations and bounds for eigenvalues of elliptic operators", *SIAM J. Numer. Anal.* **4** (1967) 89–102; doi:10.1137/0704008.

[26] D. Gaier, *Lectures on complex approximation* (Birkhäuser, Basel, 1987).

[27] W. Gander and J. Hřebíček, *Solving problems in scientific computing using Maple and MATLAB*, 4th edn (Springer, Berlin, Heidelberg, 2004).

[28] J. B. Garnett and D. E. Marshall, *Harmonic measure* (Cambridge University Press, Cambridge, 2005).

[29] C. C. Green, M. A. Snipes and L. A. Ward, "Using the Schottky–Klein prime function to compute harmonic measure distribution functions of a class of multiply connected planar domains", ANZIAM Conference 2018, 8 February 2018; http://www.maths.utas.edu.au/anziam2018/documents/ANZIAM2018Handbook.pdf.

[30] C. C. Green, M. A. Snipes and L. A. Ward, "Harmonic measure distribution functions for a class of multiply connected symmetric slit domains", March 2018, In preparation.

[31] L. Greengard and V. Rokhlin, "A new version of the fast multipole method for the Laplace equation in three dimensions", *Acta Numer.* **6** (1997) 229–269; doi:10.1017/S0962492900002725.

[32] W. Hackbusch, *Hierarchical matrices: algorithms and analysis* (Springer, Berlin–Heidelberg, 2015).

[33] J. Helsing and R. Ojala, "On the evaluation of layer potentials close to their sources", *J. Comput. Phys.* **227** (2008) 2899–2921; doi:10.1016/j.jcp.2007.11.024.

[34] P. Henrici, "A survey of I. N. Vekua's theory of elliptic partial differential equations with analytic coefficients", *Z. Angew. Math. Phys.* **8** (1957) 169–203; doi:10.1007/BF01600500.

[35] R. W. Hockney, "A solution of Laplace's equation for a round hole in a square peg", *J. SIAM* **12** (1964) 1–14; doi:10.1137/0112001.

[36] L. V. Kantorovich and V. I. Krylov, *Approximate methods of higher analysis* (Interscience, New York, 1960).

[37] A. Karageorghis and G. Fairweather, "The method of fundamental solutions for the numerical solution of the biharmonic equation", *J. Comput. Phys.* **69** (1987) 434–459; doi:10.1016/0021-9991(87)90176-8.

[38] V. Kupradze, *Potential methods in the theory of elasticity* (Israel Program for Scientific Translations, Jerusalem, 1965).

[39] J. Liesen, O. Sète and M. Nasser, "Fast and accurate computation of the logarithmic capacity of compact sets", *Comput. Methods Funct. Theory* **17** (2017) 689–713; doi:10.1007/s40315-017-0207-1.

[40] N. H. Malik, "A review of the charge simulation method and its applications", *IEEE Trans. Elect. Insul.* **24.1** (1989) 3–20; doi:10.1109/14.19861.

[41] C. B. Moler, "Accurate bounds for the eigenvalues of the Laplacian and applications to rhombical domains", Technical Report CS 121, Department of Computer Science, Stanford University, 1969, http://i.stanford.edu/pub/cstr/reports/cs/tr/69/121/CS-TR-69-121.pdf.

[42] M. M. S. Nasser, "Fast solution of boundary integral equations with the generalized Neumann kernel", *Electron. Trans. Numer. Anal.* **44** (2015) 189–229; https://www.researchgate.net/publication/256097368_Fast_solution_of_boundary_integral_equations_with_the_generalized_Neumann_kernel.

[43] M. M. S. Nasser and C. C. Green, "A fast numerical method for ideal fluid flow in domains with multiple stirrers", *Nonlinearity* **31** (2018); 815–837; doi:10.1088/1361-6544/aa99a5.

[44] M. M. S. Nasser, A. H. M. Murid, M. Ismail and E. M. A. Alejaily, "Boundary integral equations with the generalized Neumann kernel for Laplace's equation in multiply connected regions", *Appl. Math. Comput.* **217** (2011) 4710–4727; doi:10.1016/j.amc.2010.11.027.

[45] H. Ogata and M. Katsurada, "Convergence of the invariant scheme of the method of fundamental solutions for two-dimensional potential problems in a Jordan region", *Jpn. J. Ind. Appl. Math.* **31** (2014) 231–262; doi:10.1007/s13160-013-0131-3.

[46]   T. J. Price, T. Mullin and J. J. Kobine, "Numerical and experimental characterization of a family
       of two-roll-mill flows", *Proc. R. Soc. Lond.* A **459** (2003) 117–135; doi:10.1098/rspa.2002.1022.

[47]   W. J. Prosnak, *Computation of fluid motions in multiply connected domains* (G. Braun, Karlsruhe,
       1987).

[48]   T. Ransford, *Potential theory in the complex plane* (Cambridge University Press, Cambridge,
       1995).

[49]   T. Ransford and J. Rostand, "Computation of capacity", *Math. Comp.* **76** (2007) 1499–1520;
       doi:10.1090/S0025-5718-07-01941-2.

[50]   Lord Rayleigh, "On the influence of obstacles arranged in rectangular order upon the properties of
       a medium", *Phil. Mag.* **34** (1892) 481–502; doi:10.1080/14786449208620364.

[51]   J. Rostand, "Computing logarithmic capacity with linear programming", *Exp. Math.* **6** (1997)
       221–238; doi:10.1080/10586458.1997.10504611.

[52]   C. Runge, "Zur Theorie der eindeutigen analytischen Functionen", *Acta Math.* **6** (1885) 229–244;
       doi:10.1007/BF02400416.

[53]   C. Runge, "Uber empirische Funktionen und die Interpolation zwischen äquidistanten Ordinaten",
       Z. Math. Phys. **46** (1901) 224–243.

[54]   H. Singer, H. Steinbigler and P. Weiss, "A charge simulation method for the calculation of high
       voltage fields", *IEEE Trans. Pow. App. Syst.* **5** (1974) 1660–1668;
       doi:10.1109/TPAS.1974.293898.

[55]   L. N. Trefethen, "Ten digit algorithms", *Numer. Anal. Rep. 05/13*, Oxford U. Computing
       Lab., 2005, https://protect-au.mimecast.com/s/MwT8CoVzE9HKDkzgsViQE4?domain=people.
       maths.ox.ac.uk.

[56]   L. N. Trefethen, *Approximation theory and approximation practice* (SIAM, Philadelphia, PA,
       2013).

[57]   J. L. Walsh, "The approximation of harmonic functions by harmonic polynomials and by harmonic
       rational functions", *Bull. Amer. Math. Soc. (N.S.)* **35** (1929) 499–544;
       doi:10.1090/S0002-9904-1929-04753-0.

[58]   F. Záviška, "Über die Beugung elektromagnetischer Wellen an parallelen, unendlich langen
       Kreiszylindern", *Ann. Phys.* **345** (1913) 1023–1056; doi:10.1002/andp.19133450511.